Au/Fe thin-film magnetic multilayer materials: A layer-specific structural analysis using medium-energy ion scattering

T. C. Q. Noakes* and P. Bailey
CCLRC Daresbury Laboratory, Daresbury, Warrington WA4 4AD, United Kingdom

P. K. Hucknall, K. Donovan, and M. A. Howson
Department of Physics, University of Leeds, Leeds LS2 9JT, United Kingdom
(Received 29 January 1998)

This paper presents an account of the application of medium-energy ion scattering (MEIS) to the investigation of thin-film metallic multilayers grown using molecular-beam epitaxy. MEIS can provide high resolution compositional and structural information as a function of depth in the near surface region (0–250 Å); these parameters are inextricably linked with the magnetic properties exhibited by materials of this type. Amongst the information available from MEIS is the accurate determination of the layer spacings, structural information from individual layers (even at thicknesses close to a monolayer), and high sensitivity to disorder in the layers. MEIS therefore provides additional information above that provided by *in situ* reflection high-energy electron diffraction monitoring during growth and *ex situ* x-ray diffraction measurements so that it represents an ideal complementary technique for the analysis of thin-film magnetic multilayer materials of this type. An Au/Fe multilayer sample of a type previously shown to exhibit giant magnetoresistance (GMR) was analyzed. Individual gold layers were clearly resolved and a measurement of the bilayer spacing obtained; this parameter determines the magnitude of the exchange coupling and GMR. Au/Fe/Au trilayer samples grown on both MgO(100) and sapphire(1120) substrates were also analyzed for a series of Fe layer thicknesses between 2 and 16 Å. The MgO(100) grown samples showed unusually high second-layer Au signal consistent with atomic layer spacings in the Fe layers that lead to enhanced illumination of the second-layer Au. This effect could be modeled using bcc(100) layer spacings thus confirming the structure to be bcc(100) Fe between fcc(100) Au layers. In the sapphire-grown samples, twinned fcc(111) structure was observed in the individually resolved Au *and* Fe layers. The amplitude of the Fe blocking features was reduced with increasing Fe layer thickness indicating a reduction in crystallinity until for the highest thickness there was little indication of structure within the layer. The maximum layer thickness for fcc(111) Fe growth was seen to lie between 8 and 16 Å. [S0163-1829(98)06131-1]

I. INTRODUCTION

The ability to obtain structural information from the surface and subsurface region of metallic materials is extremely important for the investigation of layered magnetic structures grown by techniques such as molecular-beam epitaxy (MBE). An array of both *in situ* and *ex situ* techniques already exists to obtain chemical and structural information, with the most widely used structural techniques being reflection high-energy electron diffraction[1–4] (RHEED) and x-ray diffraction (XRD).[2–4] However, these techniques have limitations if the layer structure to be investigated is in the near-surface region, i.e., less than 250 Å below the surface of the material. RHEED only examines the outermost atomic layer and in x-ray diffraction the layers should generally occupy some fraction of the extinction depth. Further, a number of other surface structural and chemical techniques (e.g., Auger electron spectroscopy, x-ray photoelectron spectroscopy, low-energy electron diffraction) are available, but their penetration distance into the material is limited by the mean free path of the emerging electrons, typically 10–20 Å. Conventional Rutherford backscattering measurements are resolution limited by the detector to about 50–100 Å (Ref. 5) and although the use of grazing incidence may significantly improve this,[6] a fixed experimental geometry also limits the amount of structural information that can be obtained. Clearly there exists a region of about 100 Å from which information is difficult to obtain. Medium-energy ion scattering (MEIS) has the unique ability to provide a combination of compositional and structural information in this region with close to layer-by-layer depth resolution. This technique has for several years been used in the study of surface and near-surface composition and structure,[7–9] although applications seem principally to have been limited to the study of semiconductor layered structures,[10] with very little application to metallic thin-film multilayer materials such as those discussed here.[11,12]

Ion scattering techniques rely on an analysis of the products of binary collisions between incident ions and positive cores of the atoms that compose the near-surface region.[9] The resultant energy of the scattered particles can be calculated from the scattering angle and the masses of the atoms involved using well-understood kinematic relationships; hence it is possible to determine the mass of atoms in the near-surface region. Also, as the incident ion penetrates the material, it loses energy due to inelastic loss processes and the energy of the backscattered ions is reduced proportionally; hence it is possible to distinguish those scattered particles that result from surface collisions from those that originate deeper within the material. In addition, changes in

scattered ion intensity as a function of angle give crystallographic information about the material. This arises from either channeling or blocking caused by the arrangement of the atoms preventing in-going or scattered ions traveling along particular orientations within the solid.

In the past 10 years a great deal of work has been carried out in the field of thin-film magnetism. Much of this work has concentrated on the study of multilayered structures, since they exhibit magnetic properties such as ''giant magnetoresistance'' (GMR). Within this field Fe/Au multilayered structures have been extensively studied, because of the existence of the exchange coupling effects that give rise to the GMR phenomenon.[2,13] Since differences in the structure of these multilayered materials is expected to influence the magnetic properties of the films, a detailed investigation of the relationship between structure and growth conditions should provide valuable information, which may in the long term lead to the production of better quality materials exhibiting enhanced properties.

The growth of Fe on Au(100) substrates is fairly well understood,[1,2] with the Fe layers able to grow in a bcc configuration with a very small lattice mismatch (around 0.6%) if a lattice rotation of 45° is allowed. However, there are conflicting results as to how Fe grows on Au(111) substrates, especially for films around 10 Å thick.[3,14,15] Above this thickness bcc growth will again occur,[3] but below this value the Fe is thought to adopt the fcc structure of the substrate.[14] In this paper, a series of Fe thin films grown on both Au(100) and Au(111) are investigated, which demonstrate that structural and compositional information can be obtained from the subsurface layers of interest.

II. EXPERIMENT

A. MBE

MBE is an important tool for the production of materials of this type due to its highly controllable growth conditions and ability to produce atomically flat surfaces. All the samples used in this experiment were grown at Leeds in the VG-80M MBE system with a base pressure of 4×10^{-11} mbar. Deposition rates were calibrated using a quartz film thickness monitor and typical growth rates were around 0.2 Å/s. The principal diagnostic for samples during growth was a 15 kV RHEED gun operated in conjunction with a KSA 300 data collection system.

Three separate types of samples were grown: a single Fe/Au multilayer sample on a MgO(100) substrate, Au/Fe/Au trilayer samples on MgO(100), and Au/Fe/Au trilayers on sapphire(1120). Schematic diagrams showing the layer structure of the samples are given in Fig. 1. Growth conditions for each of these types will now be discussed separately.

1. Multilayer sample

The multilayer sample was grown on a MgO(100) substrate with a 10 Å Fe seed layer and a 200 Å Au buffer grown at 200 °C. The multilayer structure comprised 20 repeats of 22 Å of Fe and 10 Å of Au grown at room temperature, with the last Au layer acting as the cap. In this configuration the Au buffer layer is expected to grow as fcc(100), the Fe layers are expected to form bcc(100), and the Au layers are expected to adopt an fcc(100) configuration.[2,3] The RHEED patterns observed during growth appeared to confirm this growth behavior. Samples grown under identical conditions have been shown to exhibit varying degrees of exchange coupling as evidenced by GMR measurements with a maximum value of 40% depending on the Fe layer spacing.[16]

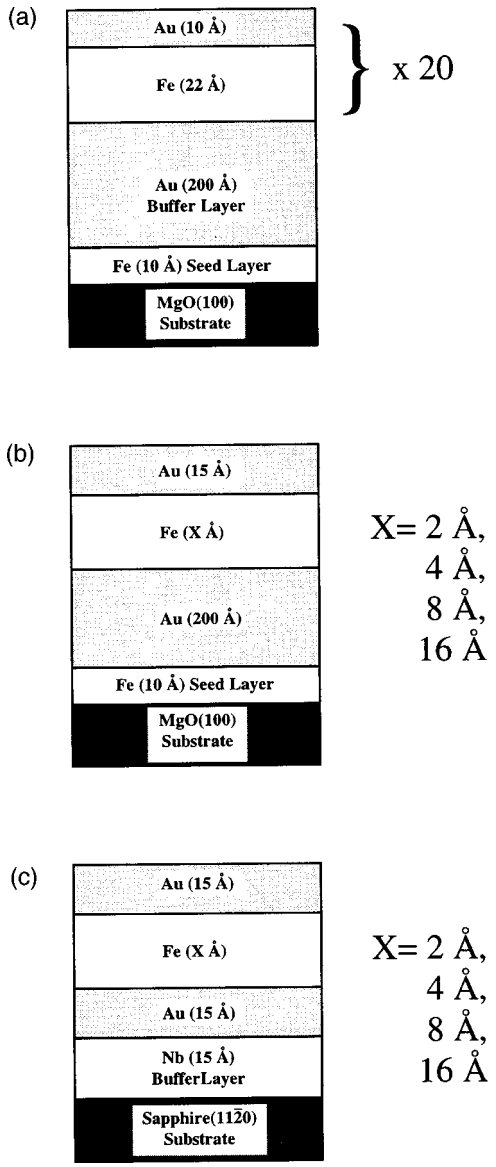

FIG. 1. Schematic representations of the samples analyzed using MEIS. (a) 20-period multilayer structure grown on MgO [exhibiting (100)-type growth surface], (b) MgO-grown trilayer samples, (c) sapphire-grown trilayer samples [exhibiting (111)-type growth surface].

2. MgO trilayer samples

Trilayer samples were also grown on MgO(100) substrates, again with a 10 Å Fe seed layer and a 200 Å Au buffer. An Fe film of either 2, 4, 8, or 16 Å thickness was then deposited followed by a 15 Å Au capping layer. Here again, the Au buffer grows as fcc(100), the Fe is expected to form bcc(100) with the capping layer also adopting an

fcc(100) configuration. Again RHEED patterns consistent with the expected growth behavior were observed throughout the growth process.

3. Sapphire trilayer samples

The sapphire trilayer samples were grown on the $(11\bar{2}0)$ surface of single-crystal substrate with a 15 Å Nb buffer layer. The Nb buffer exhibits bcc(110) structure and has a low lattice mismatch with the Au buffer layer, which in turn exhibits fcc structure with a (111)-type growth surface.[2] On top of the Nb buffer a 15 Å Au film was deposited, followed by an Fe layer to the required thickness of either 2, 4, 8, or 16 Å and finally a 15 Å Au capping layer. Despite the absence of a thick Au buffer layer between the Nb and Fe layers, RHEED indicated sixfold symmetry typical of a (111)-type surface throughout both gold layers and the thin Fe film, consistent with fcc growth.

Prior to analysis, samples were stored and transferred in a low vacuum system and briefly exposed to atmosphere during transfer into the MEIS apparatus.

B. MEIS

Ion scattering experiments were carried out using the Daresbury MEIS facility. For these experiments a 100 keV He^+ ion beam was employed with a current of up to 1 μA and a dose per data set of 5 μC. The angle and energy of the scattered ions are determined using a state-of-the-art toroidal electrostatic energy analyzer with position-sensitive detector. This allows the simultaneous collection of ions from a 24° range of scattering angles and with a range of energies equal to 2% of the pass energy. The raw data are thus in the form of a two-dimensional (2D) array of intensity as a function of energy and angle. A complete data set is constructed from several 2D arrays of different angles and energies and several examples are shown in the results section. The variation of backscattered ion intensity over the angular and energy range is shown by a false color map using the visible spectrum from violet to red to indicate increasing intensity.

The 2D data can be sectioned to produce a 1D angle spectrum (or 1D energy spectrum). The 2D data can also be processed to ''gate'' a range of energies that vary with angle, so that the signal from a specific element and/or layer can be isolated from other elements or layers. Examples of 1D angle spectra (blocking patterns) from specific layers within the samples analyzed are also shown and discussed in the results section. The blocking dips seen in these spectra can be attributed to known crystallographic orientations within the samples. The ratio of the intensity in blocking and nonblocking geometries (amplitude of the blocking dip) can be used as a relative measure of the degree of crystallinity in each layer.

Another type of data set presented here is the azimuthal scan, which involves rotation about the sample normal whilst integrating the detector counts from some area of the detector (often the entire area). By setting the analyzer energy to correspond to signal from a particular element or layer information can be obtained about the structure of that element or layer. Scans of this type are also used in conjunction with similarly collected scans of in-plane and out-of-plane incidence angle to align the samples prior to collection of the 2D data sets.

III. RESULTS AND DISCUSSION

A. Multilayer sample

This sample was chosen as an example of a practical Fe/Au multilayer that exhibits the GMR phenomenon. Figure 2 shows a full 2D data set for this sample taken using a [110] incidence geometry (45° off normal in a ⟨100⟩ azimuth). A series of bands of intensity can be seen from high energy to much lower energy, arising from the contributions of each individual Au layer to the scattering spectrum. In total, about 4–5 bands can be resolved with the modulation decreasing in intensity as the energy decreases. This decrease arises due to straggling effects in the inelastic energy losses; it is this phenomenon that effectively limits the probing depth of the MEIS technique. However, despite straggling, information is available from the resolvable layers and the energy separation of the bands can be used in conjunction with the path length and stopping power to obtain an independent calibration of the periodicity of the multilayer sample. The value of 34 ± 1 Å calculated from the path length of $2\sqrt{2} \times$ depth and 31 eV/Å stopping power[17] is close to the value of 32 Å predicted from the growth conditions. Whilst this value strictly represents the distance between Au layers, it also describes the periodicity of the Fe layers, which is of great importance since it determines the magnitude of the exchange correlation effect and the observed GMR.[2] Whereas the layer repeat distance obtained from growth is inferred from the deposition rates and exposure times, the value derived from MEIS is an actual measurement of this parameter. The precision is dominated by the accuracy with which the energy loss for each layer can be determined and is therefore high due to the good energy resolution of the instrument. There are potential problems associated with the use of semiempirical stopping powers that strictly apply to random materials, since in single-crystal channeling orientations the stopping power can vary from the random value.[18] However, in this experiment a comparison of the energy loss in both blocking and random exit geometries suggests that no significant variation in the stopping power occurs, probably because the sample is not a perfect crystal.

In addition, the 2D spectrum from the multilayer sample shows clear evidence of blocking dips that confirm the crystalline nature of the epitaxially grown layers. The large amplitudes of the blocking dips (approximately 30%) show that the degree of crystallinity is high. MEIS is also sensitive to strain-induced distortion in layered materials of this type, although in this case the angles between the [111] channel (surface normal) and [110] channel demonstrate no tetragonal distortion within the resolution limit of 1%. Strain-induced distortion is not expected for this materials combination because of the very low lattice mismatch.

Figure 3 shows an azimuthal scan taken with the incidence angle held at 45° off normal (where [110]-type channeling occurs) and the energy window gated to the Au signal. Large intensity dips are seen at 45° intervals, although the periodic repeat distance is actually 90°, indicating fourfold symmetry. The epitaxial layers exhibit typical behavior of a cubic structure with a (100) surface, as expected for this materials combination and indicated by the RHEED patterns observed during growth.

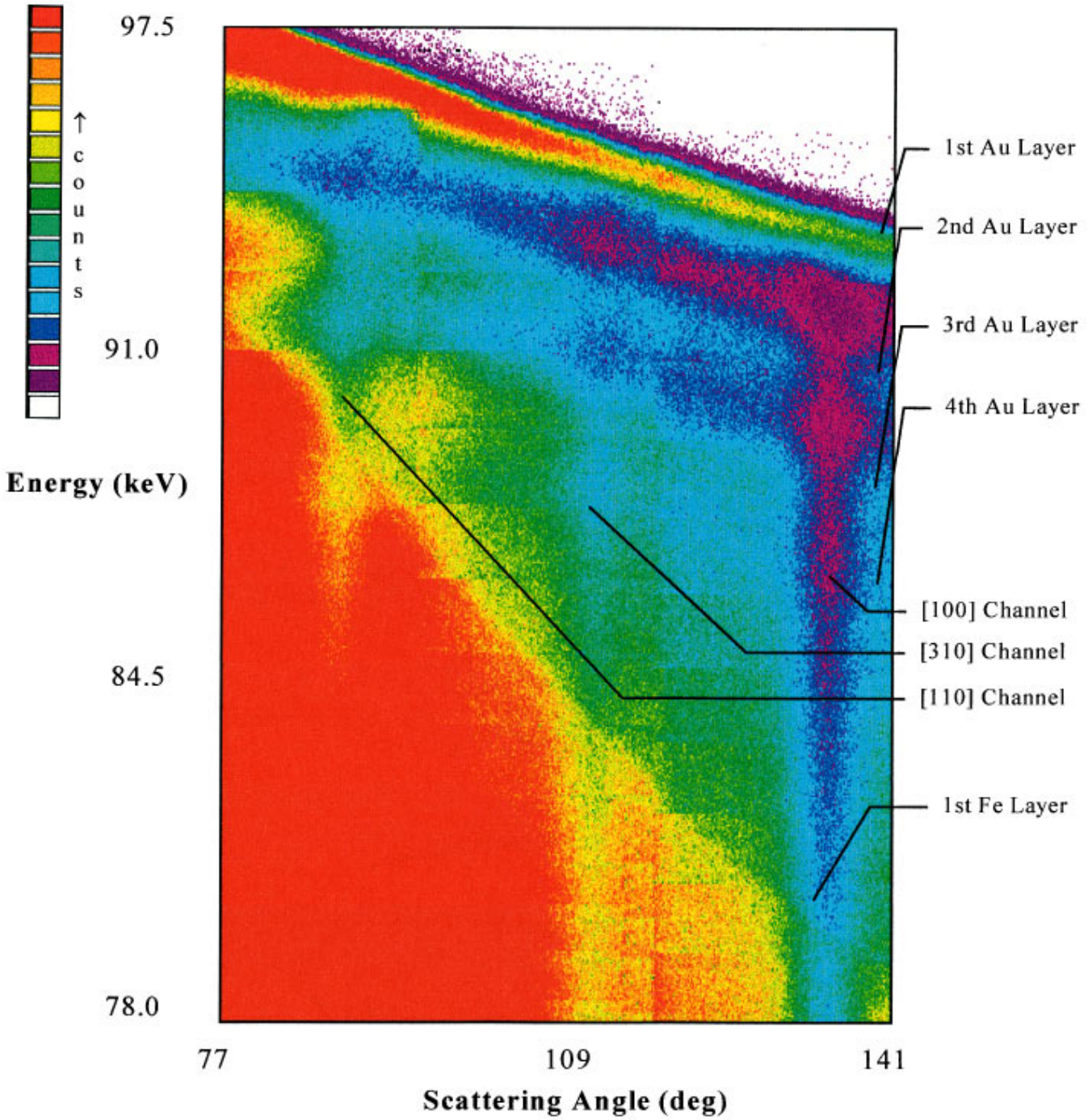

FIG. 2. (Color) A two-dimensional data set showing the variation of intensity (color scale) with scattered ion energy and scattering angle for the MgO-grown multilayer sample. The data were taken using 45° incidence along a ⟨100⟩ azimuth, which corresponds to [110]-type channeling. Up to five Au layers can be resolved (indicated by the diagonal high-intensity bands) although only one Fe band is clearly visible superimposed on an Au intensity background.

In Fig. 2, bands corresponding to the Fe are weaker in intensity (due to the lower scattering cross section) so that only one or two layers can be seen. The inability to clearly resolve the Fe layers is unfortunate since these are the layers of greatest interest, where the structure is less well understood. For this reason studies were carried out on trilayer samples specifically grown for MEIS investigation to allow the Fe intensity to be more easily resolved.

B. MgO-grown trilayer samples

Results from the MgO(100)-grown trilayer samples exhibited unusual behavior not seen in any previous MEIS studies. A data set from the 8 Å MgO grown sample is presented in Fig. 4, again using [110] incidence geometry. The presence of strong [110]-type channeling and blocking features confirms the (100) nature of the Au as expected from

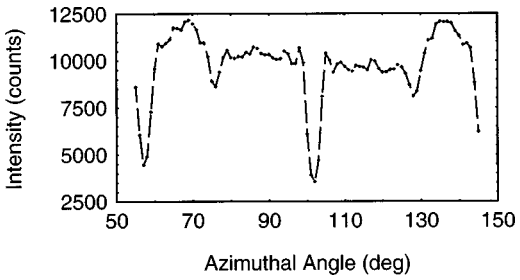

FIG. 3. An azimuthal scan of intensity from the Au signal in the multilayer sample using an incidence angle of 45°. The periodicity of 90° is consistent with a fcc(100) growth surface.

growth and indicated by RHEED. The two Au layers are well resolved and the Fe layer can be clearly seen above the Au substrate background. The most striking feature of this data set is the ''island'' of high intensity seen in the second Au layer signal in the [110] channel, with a similar but slightly less pronounced effect being seen in the Fe signal. The enhanced Au intensity can be attributed to incoherent atomic layer separations in the Au and Fe layers. The difference in atomic layer separation of the Fe with respect to the

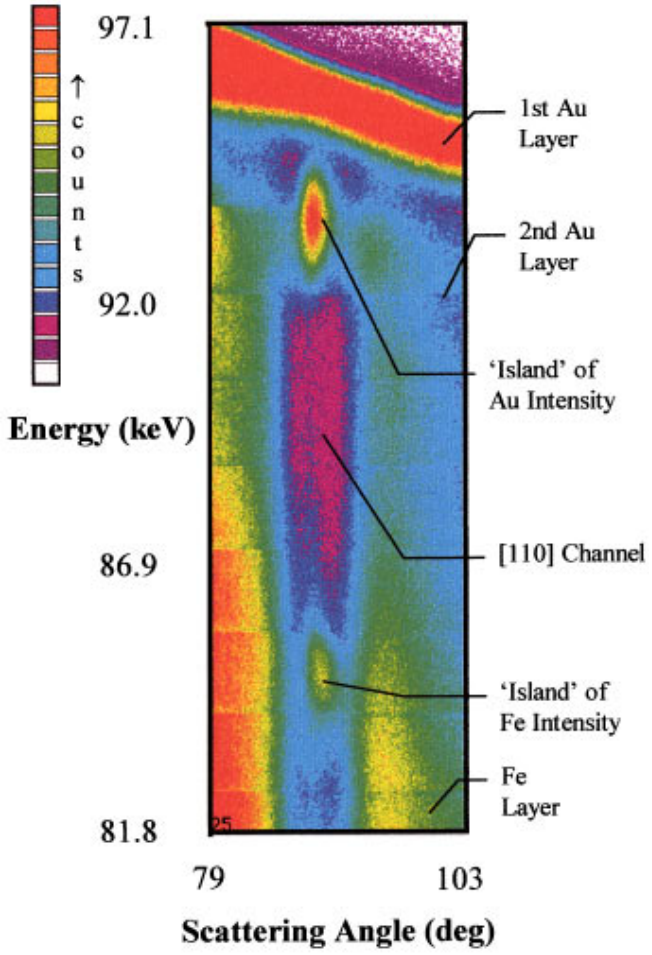

FIG. 4. (Color) A two-dimensional data set for a 8 Å Fe layer sample grown on a (100)-type substrate (using [110] incidence geometry). The islands of intensity seen in the second Au layer and Fe layer arise due to a difference in structure between the layers that leads to the Fe layer thickness being a noninteger number of Au layer spacings.

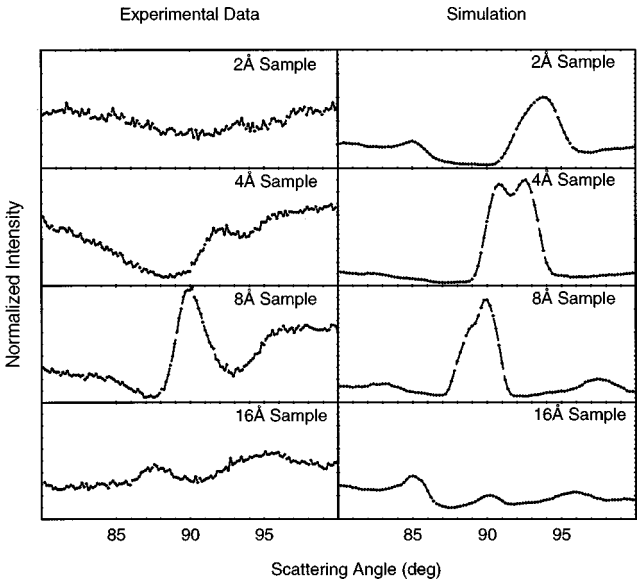

FIG. 5. Plots of the intensity in the second Au layer versus scattering angle for the (100) substrate grown samples. The island of intensity is seen to change position and size within the channel as the Fe thickness changes. The second column shows results from VEGAS simulations for the second-layer Au layer intensity. The simulations model the positions of the intensity ''islands'' well although there are some discrepancies in the size of the features.

Au effectively causes a lateral shift in the relative positions between the top Au layer and second Au layer atoms, allowing the second-layer Au atoms to be illuminated by the channeled beam. Because backscattered ions can only escape directly up an aligned channel the intensity appears only in the blocking direction where double alignment is achieved. This behavior is consistent with bulklike lattice spacings for both fcc Au and bcc Fe layers. Figure 5 shows a plot of intensity versus angle for the second Au layer of each of the four samples. The island of intensity seen in Fig. 4 moves within the channel for different Fe layer thickness as the offset between the two Au layers changes, with a maximum offset at a layer thickness of about 8 Å for the samples analyzed.

In order to confirm the interpretation of this data, the VEGAS simulation code[19] was used to generate theoretical blocking curves for comparison with experimental data. This code is more usually employed in the simulation of reconstructed surfaces, where its accuracy in modeling blocking curves is generally accepted.[7–9] A second column in Fig. 5

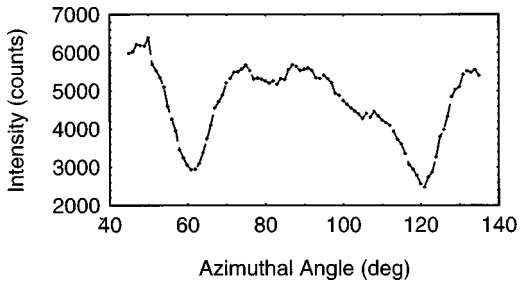

FIG. 6. An azimuthal scan of intensity from the Au signal in the 2 Å trilayer sample taken using an incidence angle of 35.3° and showing channels at a periodicity of 60°, which are consistent with two domain fcc structure and a (111)-type growth surface.

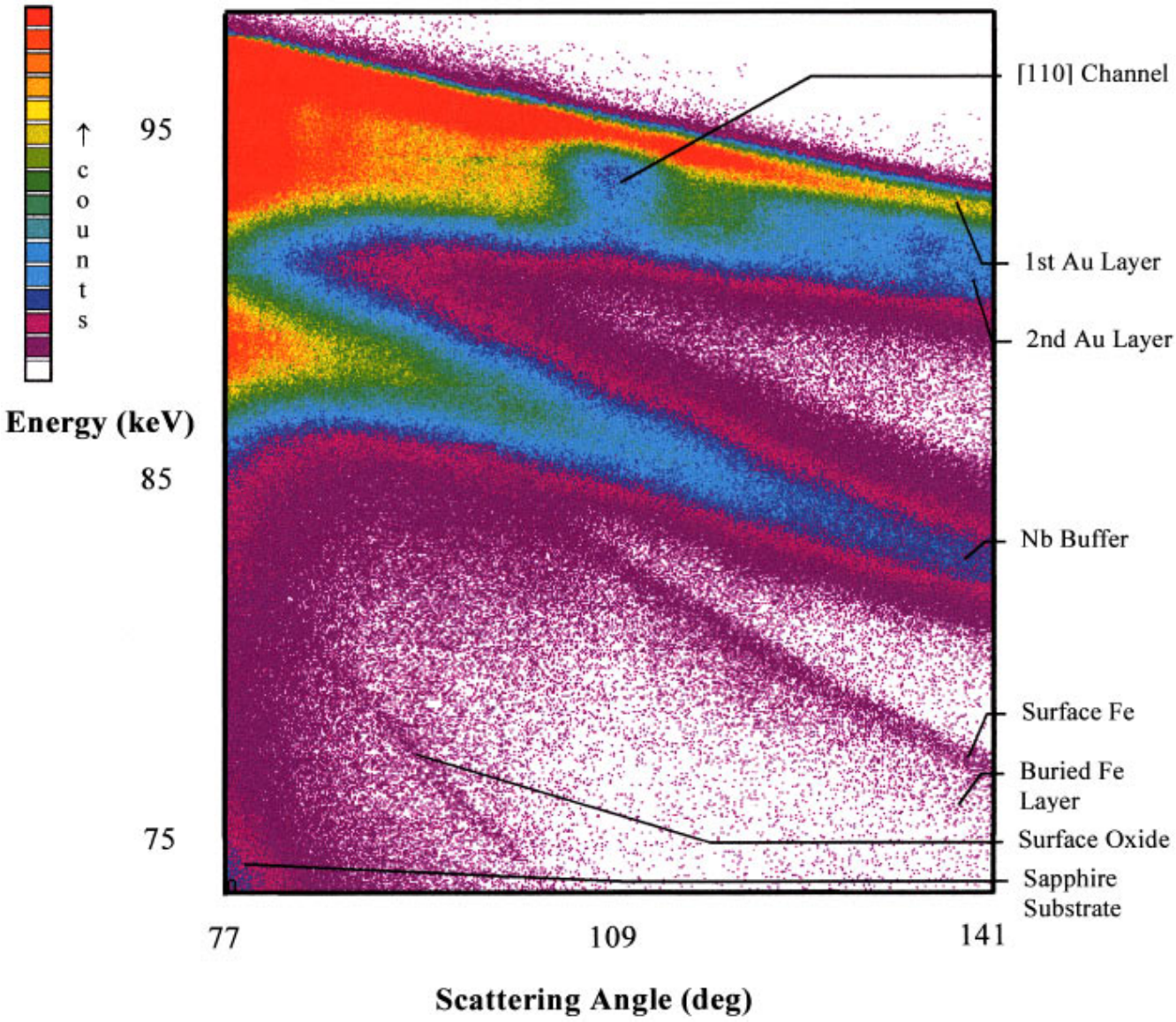

FIG. 7. (Color) A two-dimensional data set for the 2 Å Fe layer sample grown on a (111)-type substrate taken using [110]-type channeling (35.3° incidence along a ⟨211⟩ azimuth). Features arising from the different elements comprising the trilayer sample are marked. The [110] blocking dip seen in the Au signal is also present in the buried Fe signal suggesting that it has the same structure.

shows simulations of the second-layer Au intensity for each sample. The simulations were generated using bulk values for the layer spacings in the Au and Fe layers, with an intermediate value for the spacing at the two interfaces. The theory can be seen to give a good qualitative simulation of the experimental data, with the angular position of the features modeled well and consistent trends seen in both experiment and theory. The match in the absolute position of the blocking features is good, but not perfect, although this can be easily explained by errors in the actual thicknesses of the layers. However, the intensities of the features are not as well modeled, with the theory tending to overestimate the magnitude of the effect. This may be because the intensity arises from focusing effects of the ion beam in the channel, which may not be accurately modeled by the VEGAS code due to the difficulty in correctly describing the interaction potentials. The Thomas-Fermi-Moliere potentials[20] used in the simulation are better at describing the high-angle, low-impact parameter interactions involved in backscattering than the low-angle, high-impact parameter collisions involved in the channeling process. Other possible reasons for the discrepancy include a small amount of interfacial roughness or uneven layer thickness that would result in some ''smoothing'' of the effect. However, since a large amount of either of these would probably eliminate the phenomenon entirely, the existence of the ''islands'' of intensity within the blocking channel suggests a high degree of uniformity in the layers and hence the good epitaxial quality of the samples. Despite these discrepancies between experiment and the theory, the good qualitative match over a range of layer thicknesses shown in Fig. 5 is strong evidence for the bcc structure of the Fe layers. If the Fe layers were fcc in structure the samples would exhibit bulklike behavior and no additional intensity would be seen in the lower Au layer.

The Fe signal in these samples also shows intensity within the [110] channel and in this case the intensity is seen regardless of the layer thickness, since the difference in structure between the two layers means that nearly all the Fe

atoms are illuminated by the incoming ions. Although no channeling occurs within the Fe layers there is still a possibility of observing blocking in the outgoing Fe scattered ions. However, in this experiment no structural information is readily available from the Fe backscattered ions since the intensity sits on a large background of Au substrate signal.

C. Sapphire-grown trilayer samples

An azimuthal scan taken in the gold intensity of the 2 Å Fe layer sample is shown in Fig. 6 and reveals 60° periodicity in the Au layers, which is consistent with the formation of *twinned* domains of fcc with a (111)-type surface [pure (111) would give 120° periodicity]. This twinning is not detectable during growth due to the symmetry of the observed RHEED pattern. Figure 7 shows a large 2D data set for the 2 Å Fe sample taken using [110] incidence (35.3° off normal in a ⟨211⟩ azimuth). At the highest energies two diagonal bands of intensity are visible that correspond to the Au layers. Below this there is a broad band associated with the Nb buffer layer and at a lower energy the Fe intensity is seen to be separated from the buffer layer for high scattering angles. Analysis of the Fe intensity as a function of energy reveals that it is comprised of two components, with the higher-energy component being associated with material at the surface. This component has an energy width that is comparable to that of the surface O signal and this indicates that the surface Fe is present in the form of an amorphous oxide. This oxide was present for all the sapphire-grown samples analyzed, perhaps due to the relatively thin capping layer used, although its presence had not been detected prior to this study.

The Fe intensity at lower energy is associated with the buried layer. Similar energy widths were seen for the buried Fe intensity in each of the 2, 4, and 8 Å samples. Whilst the instrumental resolution (equivalent to 6 Å in this geometry) is a factor, it is probable that even with perfect resolution similar widths would be seen due to the atomic scale roughness brought about by the presence of step edges on the growth surface. Because of this effect it is not possible to rule out phenomena such as islanding of the Fe or alloy formation with the surrounding Au. However, the data are not inconsistent with the formation of homogeneous, well-defined layers of Fe in each sample. In processing the Fe intensity to produce blocking curves a ratio of approximately 2 was seen between consecutive data sets confirming the presence of the correct amount of Fe in each sample. The angular projections shown in Fig. 8 have blocking features that demonstrate periodic structure, with the main blocking feature in the Fe signal aligned in angle with the large intensity dip in the second Au layer. This arises from fcc [110]-type blocking and demonstrates the similarity in structure of the two types of layer. Figure 8 shows a comparison of the angular projections of the Fe buried layer signal for all four samples with a projection of the second Au layer from the 2 Å sample. It can be seen that the fcc [110] blocking feature is present for the 2-, 4-, and 8 Å samples, although there is an indication of reducing crystallinity within the layers as evidenced by the increase in the ratio of intensity in blocking and nonblocking orientations. For the 16 Å sample, the blocking dip has virtually disappeared suggesting very little

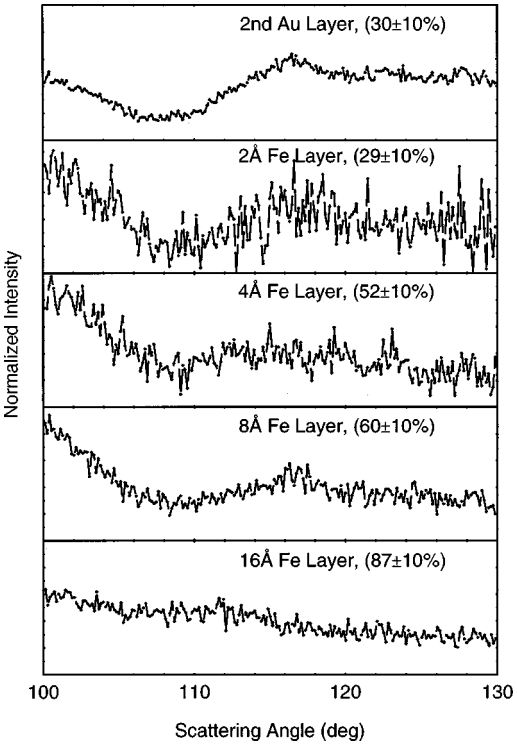

FIG. 8. Plot of the normalized backscattered intensity (obtained by dividing through by the mean) versus the scattering angle for the buried Fe layer in (111) substrate grown samples. Data are provided for four samples with different Fe layer thickness and a typical set for the second Au layer is provided for comparison. The amplitude of the blocking dip (shown in brackets for each plot) is identical in the Au layer and Fe layer of the 2 Å sample. As the Fe layer thickness increases the magnitude of the dip decreases until for the 16 Å sample there is little evidence of crystallinity.

fcc nature in this layer. These results indicate a layer thickness limit of between 8–16 Å that can be grown in a well-ordered fcc configuration.

It is apparent that MEIS is far more sensitive to disorder in these samples than the RHEED measurements made during growth. Similar well-ordered RHEED patterns were observed during growth for all four samples despite the obvious differences in epitaxial quality revealed by MEIS. In MEIS, the intensity seen within a blocking dip arises mostly from the disorder in the material, whereas the spots in a RHEED pattern arise due to the ordered fraction of the surface, with the disordered fraction contributing only to the diffuse background. This increased sensitivity to disorder represents a real advantage of ion scattering techniques over diffraction techniques such as RHEED and XRD. Whilst RHEED will remain the primary diagnostic technique used during the growth of materials of this type the value of ''*ex situ*'' measurements using MEIS has been clearly demonstrated by this investigation.

IV. CONCLUSIONS

Analysis of a Fe/Au multilayer sample showed that, although this sample was not ideal for MEIS investigation, useful information could be obtained. The sample exhibited a measured layer repeat distance of 34 ± 1 Å compared with the value of 32 Å predicted from the growth conditions.

Blocking dips revealed a high degree of crystallinity within the epitaxially grown layers and azimuthal scans demonstrated fourfold periodicity consistent with a (100) growth surface.

Data from MgO(100)-grown trilayer samples showed strong features in the backscattered intensity that are consistent with bcc(100) growth of the Fe interlayer, as expected for the materials combination used. The effect could be qualitatively modeled using the VEGAS simulation code.

Trilayer samples grown on sapphire(1120) substrates demonstrated that fcc(111) growth occurs in the Fe layer for samples with up to 8 Å of Fe, although there is a visible decrease in crystallinity with increasing Fe layer thickness. A sample with a 16 Å Fe layer exhibited very little fcc character, indicating a maximum thickness for fcc Fe growth between 8 and 16 Å.

Using MBE-grown layered samples, it has been demonstrated that the technique of MEIS can be applied to gain useful information on thin-film metallic multilayer materials. MEIS is a technique that provides a unique combination of high-resolution spectroscopic and crystallographic information. The technique has allowed an element-specific study of the structure of individual buried layers of thickness from 2 to 16 Å. Information has been gained on the thickness and structure of the layers and the degree of epitaxy within each layer. MEIS was seen to be more sensitive to disorder in the layers than the ''*in situ*'' RHEED analysis during growth and ''*ex situ*'' XRD studies commonly carried out on samples of this kind and it is therefore an ideal complementary technique.

ACKNOWLEDGMENTS

The authors wish to acknowledge the assistance of M. J. Walker in preparing the samples, and the FOM institute in Amsterdam for making available the VEGAS simulation code. Professor J. A. D. Matthew is thanked for providing encouragement and advice during the preparation of the manuscript. The Engineering and Physical Sciences Research Council is acknowledged for providing funding and access to the Daresbury MEIS facility.

*Author to whom correspondence should be addressed. Electronic address: t.c.q.noakes@dl.ac.uk

[1] Z. Celinski and B. Heinrich, J. Magn. Magn. Mater. **99**, L25 (1991).
[2] K. Shintaku, Y. Daitoh, and T. Shinjo, Phys. Rev. B **47**, 14 584 (1993).
[3] J. Xu, M. A. Howson, P. K. Hucknall, B. J. Hickey, R. Venkataraman, C. Hammond, M. J. Walker, and D. Greig, J. Appl. Phys. **81**, 3908 (1997).
[4] J. Xu, B. J. Hickey, M. A. Howson, D. Greig, M. J. Walker, and N. Wiser, J. Magn. Magn. Mater. **156**, 69 (1996).
[5] R. Hanada, M. Murayama, S. Nagata, K. Takahiro, and S. Yamaguchi, Hyperfine Interact. **84**, 171 (1994).
[6] N. P. Barradas, J. C. Soares, M. F. da Silva, F. Paszti, and E. Szilagyi, Nucl. Instrum. Methods Phys. Res. B **94**, 266 (1994).
[7] R. M. Tromp, in *Practical Surface Analysis (Second Edition) Volume 2: Ion and Neutral Spectroscopy*, edited by D. Briggs and M. P. Seah (Wiley, Chichester, 1992), p. 577.
[8] P. R. Watson, J. Phys. Chem. Ref. Data **19**, 85 (1990).
[9] J. F. van der Veen, Surf. Sci. Rep. **5**, 199 (1985).
[10] S. Sugden, C. J. Sofield, T. C. Q. Noakes, R. A. A. Kubiak, and C. F. McConville, Appl. Phys. Lett. **66**, 2849 (1995).
[11] D. E. Fowler, M. W. Hart, and J. V. Barth, Vacuum **46**, 1127 (1995).
[12] J. V. Barth and D. E. Fowler, Phys. Rev. B **52**, 1528 (1995).
[13] M. A. Howson, Contemp. Phys. **35**, 347 (1994).
[14] J. A. Stroscio, D. T. Pierce, R. A. Drogoset, and P. N. First, J. Vac. Sci. Technol. A **10**, 1981 (1992).
[15] C. Chappert, P. Bruno, B. Bartenlian, P. Beauvillain, A. Bounouh, R. Megy, and P. Veillet, J. Magn. Magn. Mater. **148**, 165 (1995).
[16] P. Ryan and B. J. Hickey, Phys. Rev. B (to be published).
[17] J. F. Ziegler, *He: Stopping Powers and Ranges in All Elements* (Pergamon, New York, 1985).
[18] Y. Kido and T. Koshikawa, J. Appl. Phys. **67**, 187 (1990).
[19] R. M. Tromp and J. F. van der Veen, Surf. Sci. **133**, 159 (1983).
[20] M. Aono, Y. Hou, R. Souda, C. Oshima, S. Otani, Y. Ishizawa, K. Matsuda, and R. Shimizu, Jpn. J. Appl. Phys., Part 2 **21**, L670 (1982).